HEALTH AND MEDICINE

Immune characterization of a xenogeneic human lung cross-circulation support system

Wei K. Wu[1,2], Matthew T. Stier[3], John W. Stokes[1], Rei Ukita[1], Yatrik J. Patel[1], Michael Cortelli[1], Stuart R. Landstreet[3], Jennifer R. Talackine[1], Nancy L. Cardwell[1], Elizabeth M. Simonds[1], Meredith Mentz[1], Cindy Lowe[4], Clayne Benson[5], Caitlin T. Demarest[1], Sophoclis P. Alexopoulos[2], Ciara M. Shaver[3]*, Matthew Bacchetta[1,6]*

Improved approaches to expanding the pool of donor lungs suitable for transplantation are critically needed for the growing population with end-stage lung disease. Cross-circulation (XC) of whole blood between swine and explanted human lungs has previously been reported to enable the extracorporeal recovery of donor lungs that declined for transplantation due to acute, reversible injuries. However, immunologic interactions of this xenogeneic platform have not been characterized, thus limiting potential translational applications. Using flow cytometry and immunohistochemistry, we demonstrate that porcine immune cell and immunoglobulin infiltration occurs in this xenogeneic XC system, in the context of calcineurin-based immunosuppression and complement depletion. Despite this, xenogeneic XC supported the viability, tissue integrity, and physiologic improvement of human donor lungs over 24 hours of xeno-support. These findings provide targets for future immunomodulatory strategies to minimize immunologic interactions on this organ support biotechnology.

INTRODUCTION

Organ transplantation has evolved to become the prevailing life-saving therapy for patients with end-stage organ failure. Despite remarkable advances on immunological, technical, ethical, and logistical fronts, the shortage of suitable donor organs remains the major challenge to meeting the demand for organ replacement (*1*). Lung transplantation is the only long-term curative therapy for patients with end-stage pulmonary disease. Over the past decade, increases in the number of lung transplants performed in the United States have largely been offset by likewise increases in the number of patients needing organ replacement, rendering waitlist mortality relatively static (*2*). The coronavirus pandemic has also brought about a subset of patients with chronic pulmonary insufficiency and a new indication for lung transplantation (*3*–*5*), and with it is a renewed urgency for approaches to expand the pool of suitable donor lungs to meet anticipated demand.

Recent estimates of available donor lung utilization remain a mere 20 to 30% (*6*–*8*). Ex vivo lung perfusion (EVLP) has emerged as an increasingly used organ preservation technique for enhanced recovery of standard and extended criteria lungs (*9*). However, duration of EVLP support in most clinical protocols and studies using acellular perfusates is limited to 6 hours (*4*, *10*, *11*). While longer duration EVLP of healthy lungs using blood-based perfusates has been reported, attempts to support injured lungs demonstrated insufficient recovery and poor performance after transplantation (*12*, *13*). More fundamentally, these isolated single-organ support systems lack the ability to replicate the complex hematologic, metabolic, endocrine, biochemical, and other homeostatic processes that enable long-term ex vivo organ support.

To overcome these limitations associated with EVLP, our group developed a cross-circulation (XC) platform capable of providing physiologic support to ex vivo donor lungs using exchange of whole blood from an organism that serves as a "host" (*14*–*18*). We showed that this system not only enabled multiday maintenance and recovery of injured porcine lungs but also supported the viability and functional recovery of human donor lungs that declined for transplantation (*16*, *17*). Nevertheless, exposure of the human lung to circulating porcine blood and xenoantigens in this system presents a potential immunologic concern upon transplant of rehabilitated lungs into human recipients. Elucidating the xenoimmunologic interactions that occur in this setting is particularly salient to future translational efforts. Thus, in this study, we profiled the immunologic sequelae of the porcine bioreactor on the human lung during xenogeneic XC.

RESULTS

Characteristics of xenogeneic XC system and donor lungs

Xeno-support swine and explanted human lungs were cannulated for xenogeneic XC, as previously described (*17*). Connection of the human lungs to the circuit and reperfusion marks the initiation of XC (Fig. 1). Characteristics of human lung donors, and EVLP parameters if applicable, are provided in Table 1. Throughout all procedures, mean organ inflow pressure at the pulmonary artery (PA) was 13.3 ± 8.8 mmHg. Xeno-support swine remained hemodynamically and biochemically stable over 24 hours of XC (mean heart rate, 98 ± 16 beats min^{-1}; systolic blood pressure, 94 ± 18 mmHg; temperature, 38.3 ± 0.9°C, and pH, 7.41 ± 0.11; figs. S2 and S3).

[1]Department of Cardiac Surgery, Vanderbilt University Medical Center, Nashville, TN, USA. [2]Department of Surgery, Division of Hepatobiliary Surgery and Liver Transplantation, Vanderbilt University Medical Center, Nashville, TN, USA. [3]Department of Medicine, Division of Allergy, Pulmonary, and Critical Care Medicine, Vanderbilt University Medical Center, Nashville, TN, USA. [4]Department of Pathology, Microbiology and Immunology, Vanderbilt University Medical Center, Nashville, TN, USA. [5]Department of Anesthesiology, Vanderbilt University Medical Center, Nashville, TN, USA. [6]Department of Biomedical Engineering, Vanderbilt University, Nashville, TN, USA.
*Corresponding author. Email: matthew.bacchetta@vumc.org (M.B.); ciara.shaver@vumc.org (C.M.S.)

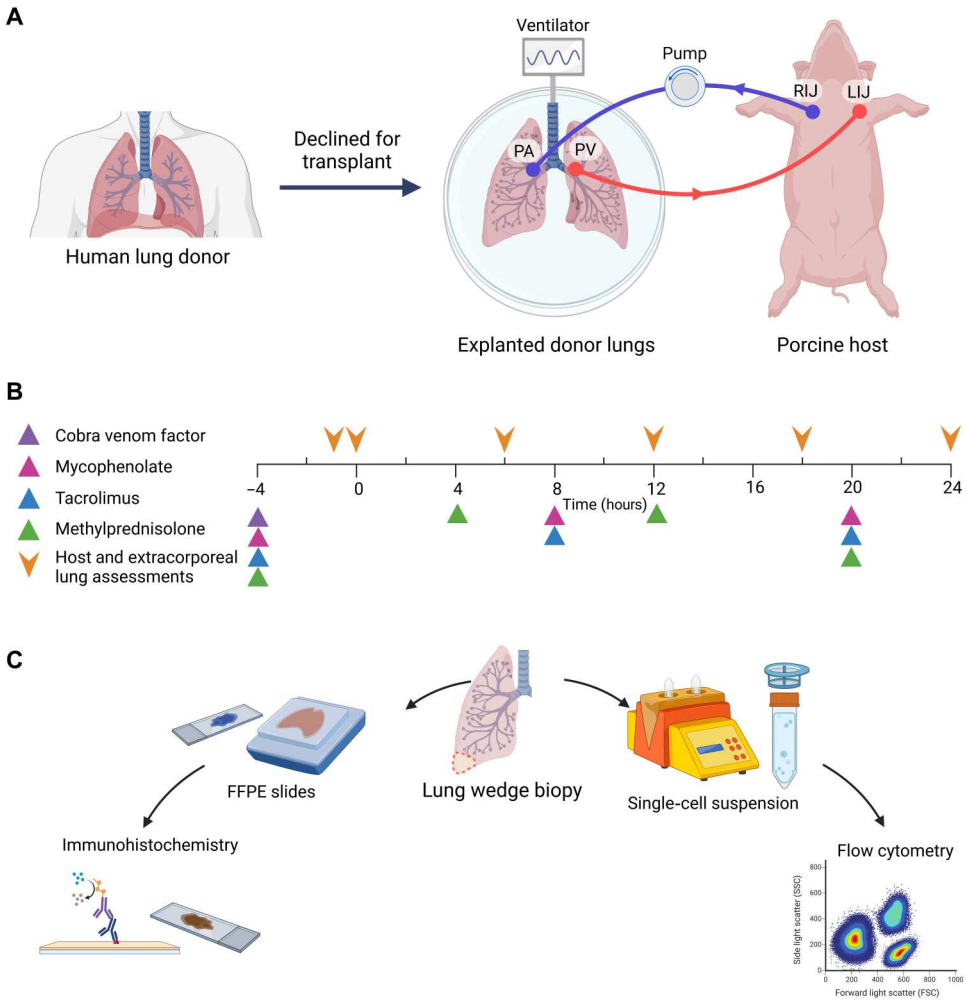

Fig. 1. Experimental design for characterization of immunologic interactions in a xenogeneic human lung XC support system. (**A**) Human donor lungs declined for transplantation were initiated on XC with an immunosuppressed, wild-type xeno-support swine. (**B**) Timeline for immunosuppression administration. Dosing: methylprednisolone 1 g (initial dose) or 125 mg (remainder doses) intravenous, every 8 hours; mycophenolate 500 mg intravenous, every 12 hours; tacrolimus 500 mg intravenous, every 12 hours; and CVF 1 mg intravenous, single dose. (**C**) Lung wedge tissue samples were collected and processed for immunohistochemistry and flow cytometry. FFPE, formalin-fixed paraffin-embedded; LIJ, left internal jugular vein; PA, pulmonary artery; PV, pulmonary vein; RIJ, right internal jugular vein; SSC, side light scatter; FSC, forward light scatter.

Characterization of cellular immune infiltration

Infiltration of porcine-derived leukocytes into the human lung during xenogeneic XC was observed (Fig. 2, A and B). Understanding the specific leukocyte populations that deposit in the human lungs will enable targeted immunomodulatory strategies to minimize immunologic injury. We performed a detailed classification of infiltrating porcine leukocytes by flow cytometry. Species-specific anti-CD45 antibodies were used to discriminate porcine and human leukocytes with high fidelity (Fig. 2C). We confirmed identification of all major myeloid and lymphoid cell populations in porcine peripheral blood mononuclear cells (PBMCs). Next, we analyzed single-cell preparations from human lungs pre-xenogeneic XC and every 6 hours during XC. We found deposition of all major leukocyte populations, with the exception of regulatory T cells, including neutrophils, monocytes/macrophages, natural killer (NK) cells, $CD4^+$ T cells, $CD8^+$ T cells, $\gamma\delta^+$ T cells, and B cells, albeit in differing proportions between lungs (Fig. 2, D to L). Marked heterogeneity existed between lungs 2, 3, and 4 in the relative frequency and timing of these porcine leukocyte infiltrates. Lung 2 had only minimal quantities of porcine leukocytes, while lungs 3 and 4 had more marked infiltration. Neutrophils represented the largest infiltrating leukocyte population (Fig. 2, D and E). There was a consistent although relatively minimal presence of monocytes/macrophages, NK cells, and $\gamma\delta^+$ T cells (Fig. 2, F, G, and K). Trace numbers of $CD4^+$ T cells, $CD8^+$ T cells, and B cells were identified, and T regulatory cells were absent (Fig. 2, H to J and L).

Characterization of antibody infiltration and complement activity

In addition to cellular infiltrates, deposition of porcine antibody in human donor lungs during XC may prime for immunopathology, particularly upon reexposure to complement sufficient human sera. Infiltration of porcine-derived immunoglobulin G (IgG) and IgM

Table 1. Demographics and clinical characteristics of human lung donors. BAL, bronchoalveolar lavage; DBD, donation after brain death; DCD, donation after cardiac death; XCC, xenogeneic cross-circulation; CT, computerized tomography.

Characteristic	Donor 1	Donor 2	Donor 3	Donor 4
Age (years)	43	43	39	16
Sex	Female	Female	Female	Male
Donor type	DBD	DBD	DCD	DBD
Single or double lung	Double	Double	Double	Double
Cause of death	Hemorrhagic stroke	Anoxic brain injury	Anoxic brain injury	Head trauma
Underlying lung disease	None	Emphysema	None	None
Smoking history (pack years)	10	48	None	None
Chest radiograph/CT findings	Right lower lobe consolidation with septal thickening, right pleural effusion	Mild centrilobular emphysema. Mild scarring in right upper lobe	Bilateral basilar airspace disease; possible small left pleural effusion; mildly enlarged main pulmonary artery	Right lung consolidation
Time on ventilator (hours)	99.8	168.4	168	125.7
Time from brain death to procurement (hours)	34.9	52.2	n/a	92.5
PaO_2/FiO_2 at time of explant (mmHg)	510	230	351	450
BAL gram stain/ fluid culture	Negative	*Staphylococcus aureus*	Mixed oral flora (sputum)	Negative
Ischemia time (hours)	16.9	17.52	21.73	37.8
Clinical EVLP before XCC (hours)	0	0	4.28	3.67
PaO_2/FiO_2 at end of EVLP	–	–	471	446

into the human lungs during xenogeneic XC was consistently observed on immunohistochemical staining (Fig. 3, A and B). Depletion of complement activity was achieved using cobra venom factor (CVF), a protein analog of complement C3. After administration of CVF, total complement activity (CH50) decreased over the ensuing 4 hours before the start of xenogeneic XC (Fig. 3C) and remained suppressed after human lung reperfusion, thus enabling maintenance of explanted lungs throughout 24 hours of xenogeneic XC.

Cytokine milieu

Cytokines regulate a cascade of nonspecific inflammation and specific immune responses following solid organ transplantation. Multiplex array quantification of plasma cytokine levels throughout XC are shown in Fig. 4 (A to L) and demonstrate greatest fold increases in interleukin-6 (IL-6; +22.7, $P = 0.001$), tumor necrosis factor–α (TNF-α; +18.46, $P = 0.01$), IL-8 (+12.8, $P = 0.04$), and IL-1 receptor antagonist (IL-1RA; +7.5, $P = 0.01$) at reperfusion, but all decreased throughout XC and approached baseline levels at the experimental end point. Interferon-γ (IFN-γ) ($P = 0.02$) and IL-12 ($P < 0.0001$) decreased throughout XC. Bronchoalveolar cytokine levels did not demonstrate significant change at experimental end point compared to baseline (Fig. 4, M to X).

Functional maintenance of human lungs

At the end point of xenogeneic XC, human lungs exhibited a partial pressure of oxygen to fraction of inspired oxygen (PaO_2/FiO_2) ratio of 420 ± 159 mmHg on 100% FiO_2, representing an increase of 242 ± 134 mmHg or 209% (Fig. 5A). Gas exchange, assessed by differences (Δ) in partial pressures of O_2 and CO_2 between blood inflow (PA) and outflow [pulmonary vein (PV)], steadily improved over 24 hours (Fig. 5, B and C). Dynamic compliance was maintained above 30 ml cmH_2O^{-1} and increased 48% over the course of XC (Fig. 5D). Peak inspiratory pressure (14.7 ± 3.6 mmHg) and plateau pressure (10.7 ± 2.8 mmHg) remained stable over the course of XC (Fig. 5E).

Lung weight remained stable or decreased throughout XC, suggesting preserved alveolar-capillary barrier integrity (Fig. 5F). Mean pulmonary flow throughout XC was 677 ± 343 ml min^{-1}. Pulmonary venous blood lactate level decreased (Fig. 5H), and swine pH remained stable (Fig. 5I) throughout XC. The number of early apoptotic cells [terminal deoxynucleotidyl transferase–mediated deoxyuridine triphosphate nick end labeling (TUNEL); Fig. 5J] decreased significantly throughout XC ($P < 0.001$), while the number of late apoptotic cells (Caspase 3; Fig. 5K) and activated neutrophils (myeloperoxidase positive; Fig. 5L and fig. S1) did not significantly change. Overall, mean changes in functional parameters over 24 hours of XC demonstrated ex vivo recovery of human lung respiratory function, consistent with previous studies (*17*).

Multiscale analyses of human lungs

After 24 hours of XC, lungs demonstrated preservation of global architecture, improved appearance of contusions, and recruitment of

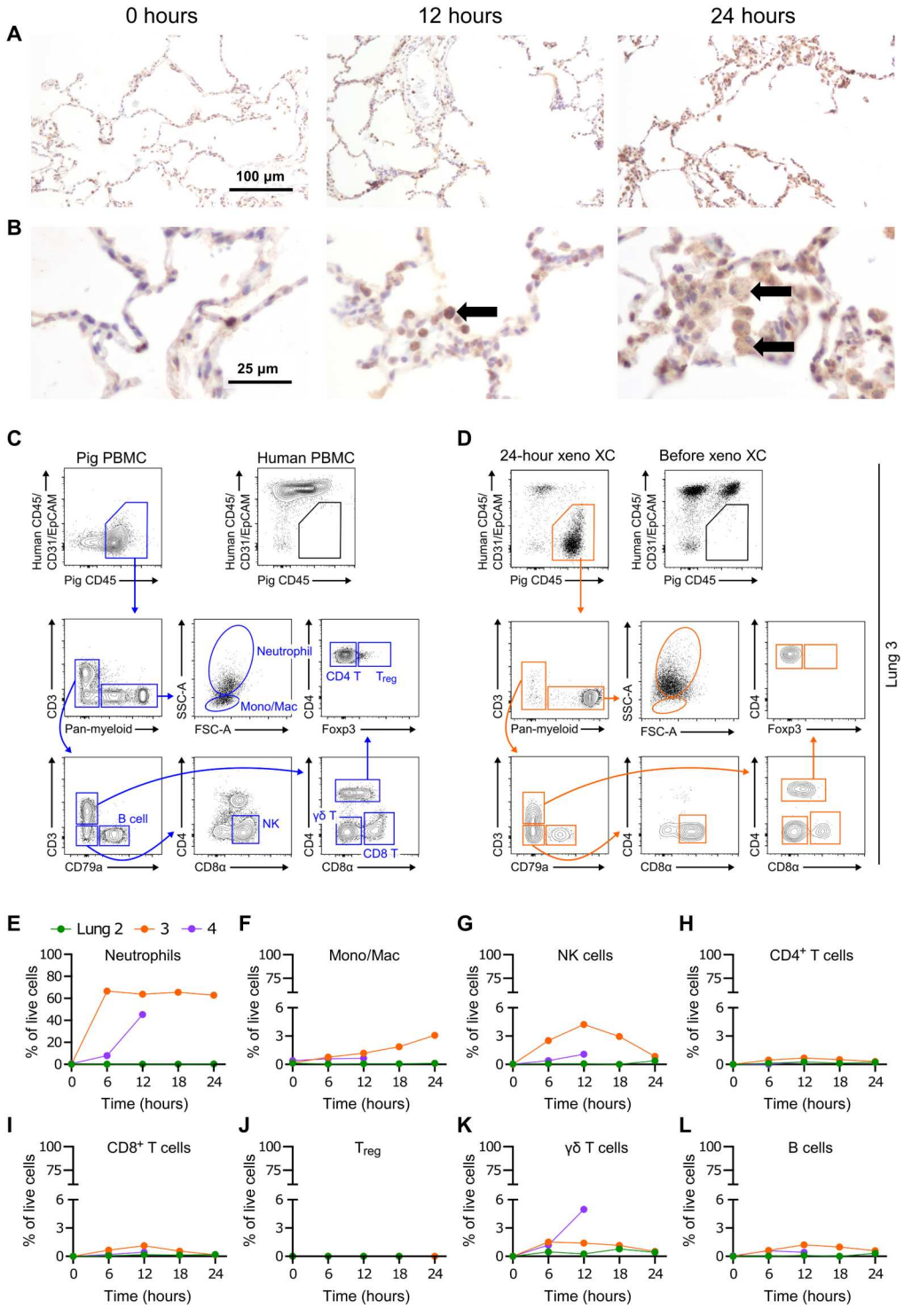

Fig. 2. Porcine immune cell infiltration in human lungs during xenogeneic XC. (**A** and **B**) Immunohistochemistry staining for porcine leukocytes (black arrows) at 0-, 12-, and 24-hour time points at low (A) and high (B) magnifications. (**C**) Gating schema for leukocyte populations in PBMCs. T_{reg}, regulatory T cell. Human PBMC shown as a specificity control. (**D**) Representative flow cytometric evaluation of infiltrating porcine-derived leukocytes at 24 hours after xenogeneic XC from single-cell preparations of lung 3 parenchyma. Pre-XC human donor parenchyma from lung 3 is shown for reference. (**E** to **L**) Porcine leukocyte populations isolated from the human lung parenchyma during xenogeneic XC, shown as percent of live cells assessed by flow cytometry. Plotted as individual lungs, specifically lung 2 (green), lung 3 (orange), and lung 4 (purple). Time point at 0 hours represents samples taken immediately before initiation of XC. All flow cytometric analyses are pregated to exclude doublets and dead cells. EpCAM, Epithelial cellular adhesion molecule; Mono, monocyte; Mac, macrophage.

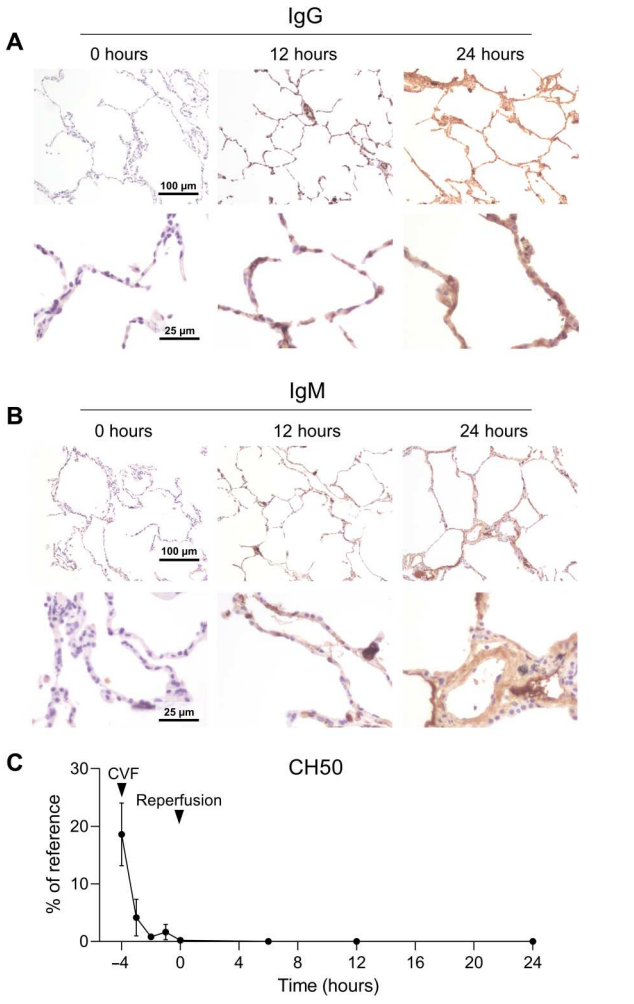

Fig. 3. Porcine Ig infiltration and complement activity during xenogeneic XC. (**A** and **B**) Immunohistochemistry staining at pre-XC (0 hours), 12- and 24-hour time points for porcine immunoglobulin G (IgG) (A) and IgM (B) deposition in human lungs. (**C**) Quantification of complement activity (CH50) before and after initiation of xenogeneic XC. CVF was administered 4 hours before initiation of XC.

consolidated segments (Fig. 6, A and B). Bronchoscopy showed normal airways without notable edema or erythema (Fig. 6C). Histologic evaluation demonstrated preservation of microscopic architecture, including alveolar organization (Fig. 6, D and E), pseudostratified epithelium in small airways (Fig. 6F), and integrity of arterioles and venules (Fig. 6, G and H). Transmission electron microscopy demonstrated intact alveolar-capillary interface (Fig. 6I) and subcellular integrity of endothelial cells (Fig. 6J) and type II pneumocytes (Fig. 6K).

DISCUSSION

We demonstrate that a porcine xenogeneic XC system is capable of supporting the viability and physiologic improvement of human donor lungs despite substantial and complex human swine immunologic interactions that occur in the context of calcineurin-based immunosuppression and complement depletion. Porcine immune cell and Ig infiltration was detected throughout XC support. However, human lungs demonstrated minimal endothelial activation and no clinical signs of acute rejection during xenogeneic XC.

Historically, the field of xenotransplantation has driven efforts toward using porcine donors as sources of transplantable organs, with most clinically relevant studies targeted towards pig-to-human xenotransplantation and preclinical investigations using pig-to–nonhuman primate (NHP) models (*19*–*22*). In these cases, the well-established and robust human immunologic reaction that leads to hyperacute rejection of the porcine organ is mediated by preformed antibodies to the αGal epitope, a carbohydrate moiety abundantly present on porcine glycoproteins and glycolipids (*23*–*25*). Binding of anti-αGal antibodies to the vascular endothelium leads to complement activation, coagulation dysregulation, thrombosis, and terminal injury (*26*).

However, the converse that a porcine recipient would mount a preformed cytotoxic response against a primate donor organ is a question that has not yet been directly investigated (*27*–*29*). In a study of porcine sera exposed to primate PBMCs, Tai *et al.* (*30*) demonstrated that pigs have natural preformed antibodies directed against human and primate PBMCs. Our group has previously demonstrated that robust immunologic rejection within 1 hour of xenogeneic XC occurs in the absence of immunosuppression and complement depletion, suggesting that preformed, porcine-derived, anti-human tissue Igs are present in swine circulation (*17*).

In this study, we demonstrate that, although rapid deposition of preformed porcine anti-human IgM and IgG ubiquitously occurs after reperfusion, as in other xenogeneic systems, human lung physiology and cytoarchitecture can still be recovered and maintained. Our data show an initial up-regulation of cytokine release and generation of a robust proinflammatory milieu. Porcine leukocyte infiltration of the human lungs occurred, with a neutrophil predominance. TNF-α, a pleiotropic proinflammatory cytokine that was elevated at reperfusion, is known to induce pulmonary transendothelial neutrophil migration in an IL-8–dependent manner (*31*, *32*). Absence of marked B cell or T cell infiltration throughout XC—cells that more likely to pose a long-term risk to the graft—suggests that the existing leukocyte infiltration is not occurring in an antigen-specific manner. However, this may also reflect the duration of xenogeneic XC, and longer periods of support may prompt more adaptive immune invasion that will need to be assessed if XC is extended to longer time points. While detrimental effects of these infiltrating porcine leukocytes cannot be fully excluded, as some of these cells (such as NK cells) (*33*, *34*) are particularly potent on a per cell basis, the majority of observed infiltrating cells have short effector half-lives (*35*). Most reassuring is the dampened inflammatory cytokine production at later time points, suggestive of a limited acute inflammatory response despite these infiltrating cells. Understanding of the specific leukocyte populations that infiltrate the human lungs will enable targeted immunomodulatory strategies to minimize immunologic injury in future studies.

Despite immune cell and antibody deposition, with appropriate immunosuppression and complement depletion, immunologic sequelae, endothelial injury, and coagulation dysregulation are limited [fig. S3 and as demonstrated in a previous study by our group (*17*)], no microthrombi are observed in tissue sections, and this type of xeno-support platform succeeds at physiologically rehabilitating the human lung while on XC with xeno-support swine. Eventual normalization of hematologic parameters and cytokine

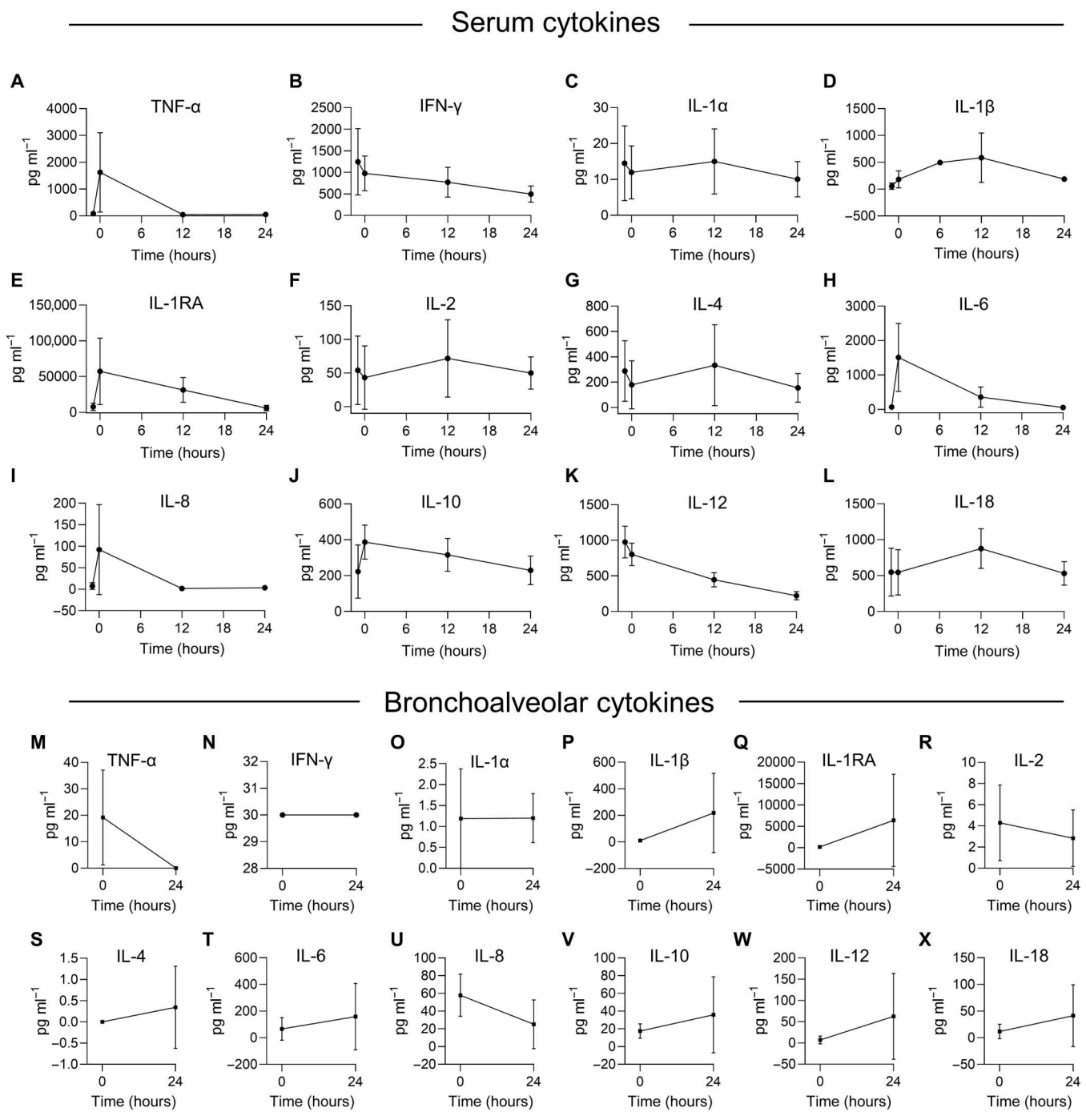

Fig. 4. Cytokine assessment during xenogeneic XC of human lungs. (**A** to **L**) Quantification of porcine plasma cytokines: TNF-α (A), IFN-γ, IL-1α, IL-1β, IL-1RA, IL-2, IL-4, IL-6, IL-8, IL-10, IL-12, and IL-18. (**M** to **X**) Quantification of human lung bronchoalveolar cytokines.

levels reflect accommodation of the human organ. Several studies have demonstrated similar instances where pig-to-NHP xenograft have survived and remained functionally intact despite evidence of antibody and complement deposition on the xenograft endothelium (*36*, *37*). The notion of accommodation, a phenomenon first described after clinical ABO-incompatible renal transplantation where allografts or xenografts acquire resistance to acute humoral injury and rejection, remains incompletely understood (*38*–*42*).

Deposition of porcine immune moieties in the human lung, although not prohibitive of organ support and rehabilitation in the current study, nevertheless poses the concern that they may have undesired immunologic consequences upon transplantation into a human recipient. Tai *et al.* (*30*) demonstrated, using a series of

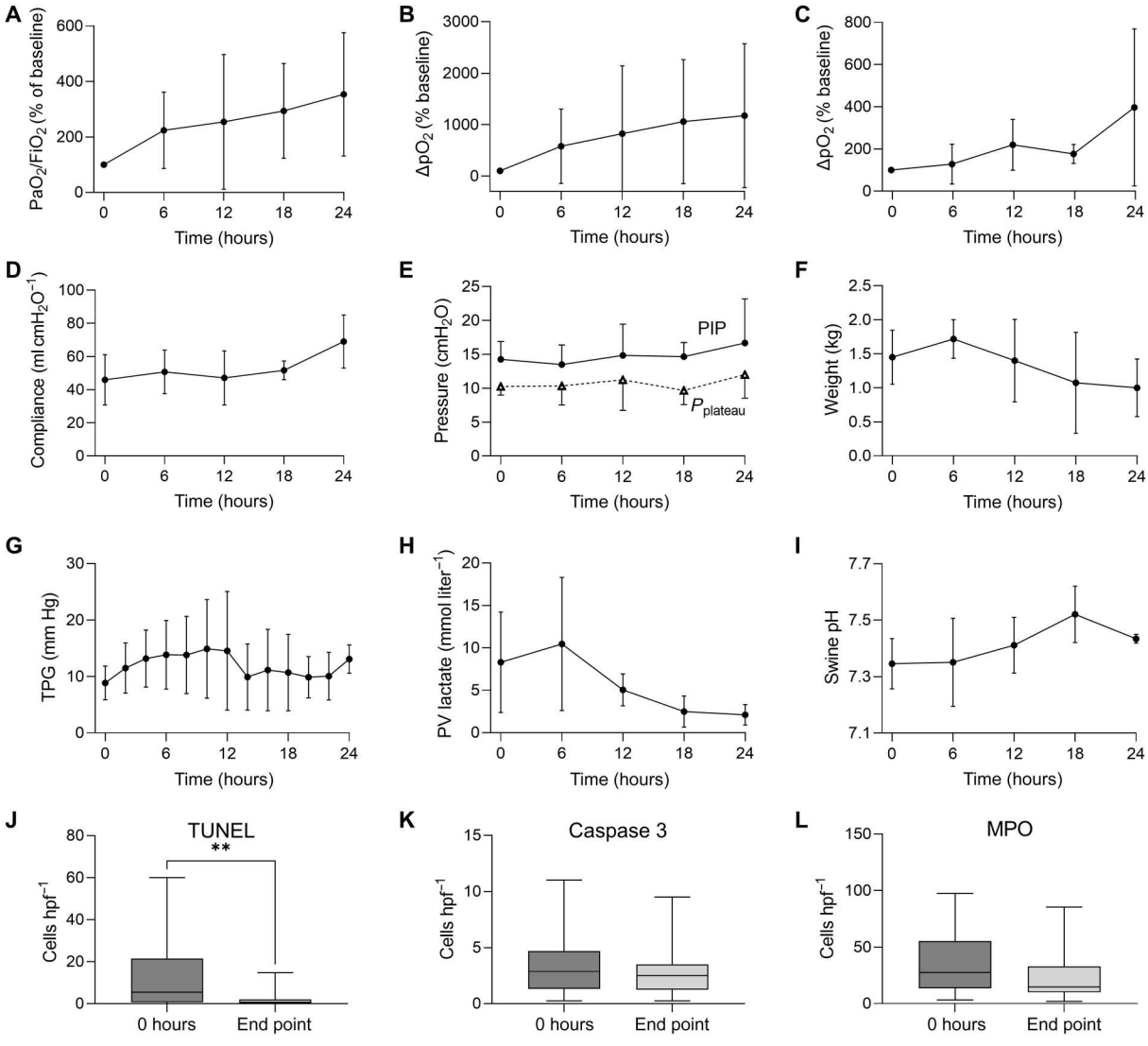

Fig. 5. Human lung function over 24-hours of xenogeneic XC. (**A**) PaO_2/FiO_2 (expressed as percent of baseline). (**B**) Change in pO_2 across lung ($\Delta p = |pPA - pPV|$; expressed as percent of baseline). (**C**) Change in pCO_2 across lung (expressed as percent of baseline). (**D**) Dynamic compliance. (**E**) Peak inspiratory pressure (PIP) and plateau airway pressure ($P_{plateau}$). (**F**) Lung weight. (**G**) Transpulmonary pressure gradient (TPG), defined as the vascular pressure difference between the PA and PV. (**H**) PV lactate concentration. (**I**) Swine arterial pH. (**J** and **K**) Changes in early TUNEL and late (Caspase 3) apoptotic markers. (**L**) Change in myeloperoxidase (MPO), a marker of neutrophil activation. hpf, high-powered field.

ex vivo mixing studies, that a porcine T cell–driven, antihuman response is possible in porcine organ xenotransplantation but postulated that the immunosuppressive therapy being administered to prevent rejection of the graft would likely suppress the anti-swine cellular response. A review of eight studies found that after exposure to porcine antigens and development of anti-porcine xenoantibodies, human recipients of a subsequent kidney or liver allograft did not develop antibody-mediated or accelerated cellular rejection (*43*). Although the immunologic implications of concurrent xeno- and allo-antigen exposure is a topic requiring further study, these findings suggest that a human organ engrafted with swine xenoantigens during xenogeneic XC could be tolerated by a transplant recipient.

The field of xenotransplantation has long endeavored to generate a source of porcine organs suitable for human transplantation. Remarkable progress in biotechnology and genetic engineering made over the last decade has enabled the creation of genetically modified pigs designed for human transplant compatibility (*22*, *44*–*47*). Despite the wave of recent progress in xenotransplantation, where multiple genetically altered porcine organs were transplanted into human body donors and a human (*46*, *48*–*50*), chronic xenoantigen exposure remains a concern for the durability of these xenografts and the risk of delayed xenograft rejection (*51*). Although most xenoreactive responses in hyperacute rejection are targeted to a few carbohydrate antigens (including αGal), innumerable species-specific antigens present on xenografts can lead to chronic exposure, rejection, and graft failure (*51*–*55*). Xenogeneic XC can circumvent the translational barriers of xenotransplantation, as exposure to the porcine biosystem and deposition of porcine immune moieties is finite and limited to the duration of XC support, thus

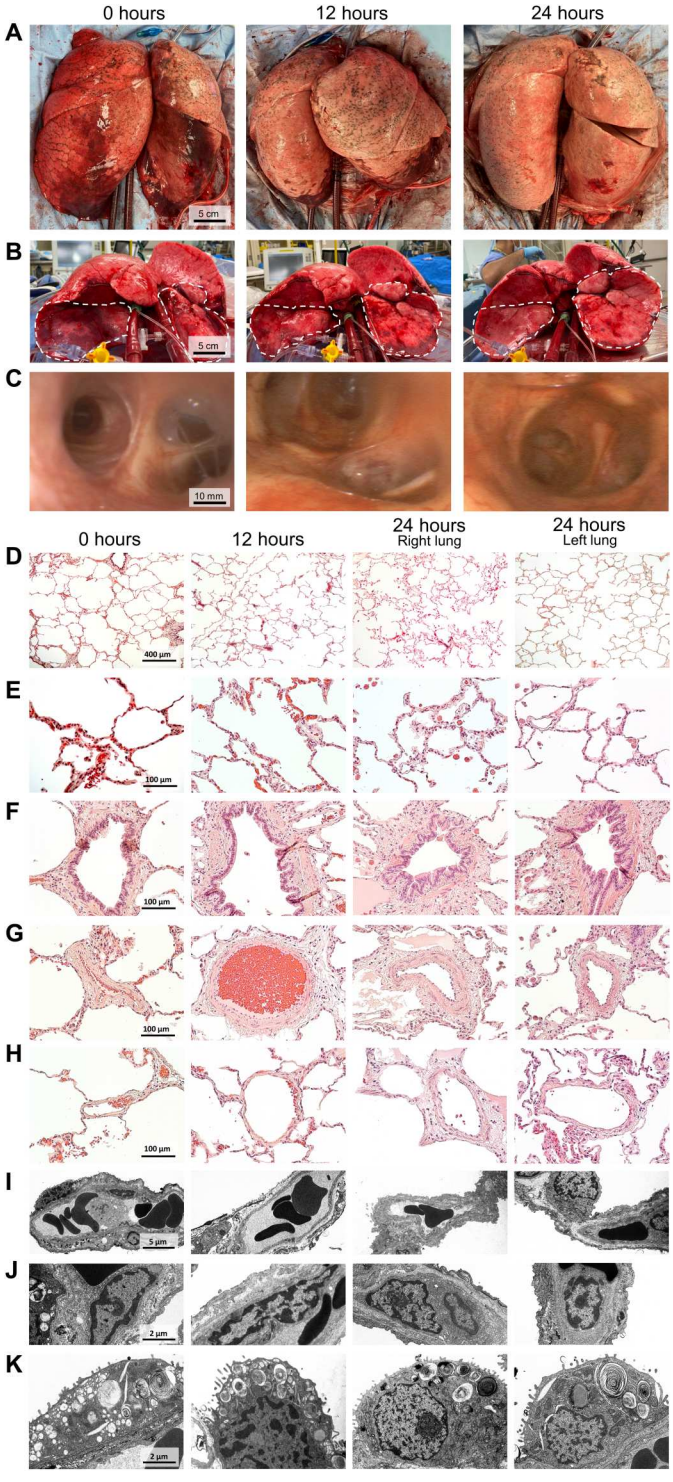

Fig. 6. Multiscale evaluations of human lungs over the course of xenogeneic XC. Gross appearance of representative dorsal lung surfaces (**A**) (lung 1) and lung bases (**B**) (lung 2) demonstrate improvement of contusions and recruitment of atelectatic regions. (**C**) Bronchographs of representative lungs. (**D** to **H**) Hematoxylin and eosin staining of lung parenchyma at low (D) and high (E) magnifications, small airways (F), arterioles (G), and venules (H). No thrombi were visualized in the examined sections. (**I** to **K**) Transmission electron microscopy of alveolar septa (I), endothelial cells (J), and type II pneumocytes (K).

opening the possibility of human lungs recovered via xenogeneic XC as possible allograft organs for human recipients. While a transient and potentially ameliorated xenoreactive response may occur against the porcine antibodies and cells, the human allograft itself may be spared from functional damage. Characterization of the immunologic interactions during xenogeneic XC reported in this study is a foundational step toward translational application of this lung recovery and rehabilitation platform.

Limitations include the number, variable pattern of injury, and differences in baseline clinical characteristics of the human lungs included in this study. In addition, lung tissue specimens were obtained without whole-organ flush. Single-cell suspensions generated from these samples may include both organ-infiltrating and circulating cells. It is possible that, if a whole-organ flush was performed, a proportion of the circulating porcine immune cells may be displaced, thus minimizing their immunologic implications on future translational efforts. Lung biopsy samples in this study were also obtained from the periphery of the organ to enable serial procurement of substantial volumes of tissue for analysis without disruption of central structures. Although there may be regional differences in ventilation or perfusion (addressed through biopsy site randomization), we do not expect substantial differences in the biologic or immunologic interactions between peripheral or central tissues. The risk of zoonotic infection during xenogeneic XC also presents a translational hurdle. While we included bacterial cultures from bronchoalveolar lavage (BAL) in this investigation, viral transmission was not evaluated, and optimal surveillance protocols remain to be fully investigated.

Reducing the deposition of porcine cellular and antibody immune agents on human lungs may (i) improve ex vivo organ rehabilitation with a decreased inflammatory milieu during xenogeneic XC and (ii) diminish immunologic reaction against porcine xenoantigens upon clinical translation. Additional pharmacologic (such as T cell–depleting therapies and IL-2 receptor antibodies) (*56*, *57*) or mechanical strategies (such as leukocyte filters) (*58*) to reduce the immunogenicity of the xenogeneic XC-recovered human organ are topics of interest for further study (Fig. 7). Use of genetically immunodeficient swine (such as antibody-deficient or severe combined immunodeficient swine) for xeno-support may be an additional adjunctive immunomodulatory strategy (*59*, *60*). Future investigation will optimize these additional techniques to reduce the immunologic interface between the human organs and xeno-support swine during xenogeneic XC, lay critical groundwork for bioengineering approaches needed for translation, and ultimately pave the way for human transplantation of xenogeneic recovered human organs.

MATERIALS AND METHODS

Animals

Yorkshire and Landrace swine (n = 4) that were 3 to 6 months of age, with a mean weight of 92 ± 13 kg (range, 61.4 to 123.0 kg) were used as xeno-support animals (Fig. 1A). The study was approved by the Institutional Animal Care and Use Committee at Vanderbilt University Medical Center and conducted in accordance with the U.S. National Research Council of the National Academies *Guide for the Care and Use of Laboratory Animals, Eighth Edition*.

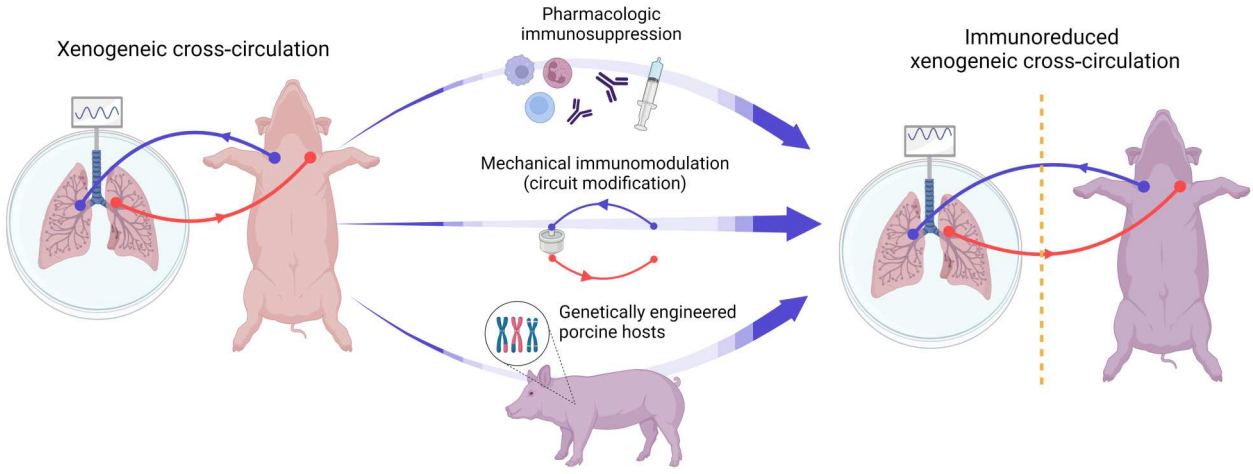

Fig. 7. Envisioned immunomodulatory strategies for use in xenogeneic XC of human lungs. Immunoreduction using pharmacologic immunosuppression, mechanical immunomodulation via circuit modification, and genetically engineered porcine host may minimize the immunologic interactions between xeno-support swine and human lungs.

Immunosuppression

To minimize the risk of immunologic rejection, an immunosuppression regimen informed by established protocols and current practices in clinical lung transplantation was used (Fig. 1B). Four hours before initiation of xenogeneic XC, xeno-support swine were anesthetized, intubated, and administered CVF (1 mg; Sigma-Aldrich) to deplete complement activity (*61*, *62*). Intravenous diphenhydramine (50 mg; West-Ward Pharmaceuticals) and methylprednisolone (1 g; Pfizer) were administered to mitigate hemodynamic instability occasionally associated with CVF. Intravenous tacrolimus (5 mg; Astellas) and mycophenolate (500 mg; Genentech) were also administered before reperfusion and redosed every 12 hours. Methylprednisolone (125 mg; Pfizer) was readministered every 8 hours after the initial dose.

Human lung donors

Donor lungs (n = 4) deemed unsuitable for clinical transplantation were procured in coordination with local organ procurement organizations under protocols approved by the Institutional Review Board at Vanderbilt University Medical Center. Informed consent for use of donor organs for research was obtained from donor families or health care proxies by local organ procurement organizations. Deidentified donor data were obtained through the United Network for Organ Sharing under approved protocols. Donors with severe purulent secretions on bronchoscopy and history of infection with HIV were excluded from eligibility.

Procurement of human lungs

When human lungs acceptable for the study were identified, a team was dispatched from Vanderbilt University Medical Center to procure lungs in accordance with standard clinical practice (*63*), in coordination with other teams deployed for organ procurement (e.g., heart, liver, and kidney) for clinical transplantation. At the time of procurement, a bolus of heparin (30,000 U) was administered intravenously, the aorta was clamped, and cold organ preservation solution (Perfadex, XVIVO) was administered through the PA as an anterograde flush. A retrograde, PV flush was also performed. Lungs were topically cooled with sterile ice slush in situ and inflated to an airway pressure of 15 cmH_2O, and the trachea was stapled. Lungs were then explanted and placed in a sterile isolation bag with 500 ml of organ preservation solution (Perfadex, XVIVO) at 4°C. The bag was placed in a second sterile isolation bag containing ice slush and subsequently placed on ice.

Lungs obtained after clinical EVLP were procured by teams from Vanderbilt University Medical Center or other academic institutions in similar fashion. After cannulation and 3 to 6 hours of standard perfusion by a commercial EVLP service (Lung Bioengineering, United Therapeutics), lungs deemed unsuitable for clinical transplantation were made eligible for research use (*64*, *65*). Post-EVLP research lungs were flushed with organ preservation solution (Perfadex, XVIVO) and transported to our study facility in static cold storage at 4°C.

Cannulation of explanted human lungs

After explant or EVLP, lungs were placed in static cold storage and transported to the research facility at Vanderbilt University Medical Center. Because of the heart being procured for clinical transplantation in all donors included in this study, segments of the structures connecting the heart and lungs (left atrial cuff and main PA) were procured with the heart, resulting in decreased tissue available for cannulation and frequent need for reconstruction of the left atrial cuff and PA (*14*, *66*). In lungs 1 and 2, donor pericardium and thoracic aorta were used to facilitate cannulation of explanted human lungs at the PA and left atrial cuff, as previously described (fig. S2) (*15*, *16*). Synthetic, funnel-shaped left atrial and PA cannulas were used for lungs 3 and 4, which were declined for transplantation after clinical EVLP by Lung Bioengineering (fig. S2) (*67*).

After reconstruction, the PA and left atrial cuffs were cannulated, and 1 liter of cold sterile isotonic electrolyte-balanced solution (Normosol, ICU Medical) was flushed through the lungs to remove preservation solution and prime the arterial and venous cannulas. The trachea was intubated with a 9-mm endotracheal tube (Medline). The lung was placed in a sterile isolation bag on an organ preservation chamber in preparation for XC.

XC between explanted human lungs and xeno-support swine

The xenogeneic XC technique has been previously described in detail (*68*). All swine participants ($n = 4$) underwent intramuscular anesthetic induction with ketamine (2.2 mg/kg; Zoetis), tiletamine (4.4 mg/kg; Zoetis), and xylazine (2.2 mg/kg; Bimeda). Anesthesia was maintained with continuous intravenous infusions of fentanyl citrate (0.03 to 0.1 mg kg^{-1} $hour^{-1}$; Hospira) and inhaled isoflurane (1 to 3% in oxygen; Henry Schein). Cefazolin (20 mg kg^{-1}; West-Ward Pharmaceuticals) and enrofloxacin (5 mg kg^{-1}; Norbrook) were administered before skin incision and readministered every 8 and 24 hours, respectively. An auricular or femoral arterial line (Arrow International) was placed for hemodynamic monitoring and periodic arterial sampling. The immunosuppression regimen was administered (Fig. 1B). Swine participants were continuously monitored by research staff throughout XC.

A heparin bolus (30,000 U; Sagent) was given, and cannulas (19 and 21 French; Medtronic) were placed in bilateral internal jugular veins under ultrasound guidance using Seldinger technique. Calcium chloride (1 g; Hospira) was administered, and explanted human lungs were connected to the circuit via cannulas secured in the PA and PV, thereby marking the start of xenogeneic XC. Perfusion circuit elements consisted of a main console (Jostra pump console, Maquet), disposable pump (Rotaflow centrifugal pump, Maquet), flexible tubing (Tygon, Saint-Gobain), and hard-shell venous reservoir (Medtronic), as previously described (*17*). Pressure and flow in the PA and PV were continuously measured real time using fluid-filled pressure transducer (TruWave, Edwards Lifesciences) and a clamp-on tubing flow probe (SONOTEC), respectively, and recorded at 400 Hz with data acquisition system (PowerLab and LabChart, ADInstruments). Throughout the duration of XC, xeno-support swine were maintained with a continuous heparin infusion. Activated clotting time (ACT) was measured using a whole-blood microcoagulation system (Hemochron, Accriva Diagnostics), and the heparin infusion was adjusted to maintain ACTs within the target range of 180 to 250 s. Physiological parameters of the xeno-support swine, including heart rate, electrocardiogram, arterial blood pressure, oxygen saturation (SpO_2), temperature, and respiratory rate were continuously monitored and recorded (figs. S3 and S4) using a multiparameter vital signs monitor (SurgiVet).

Ventilation of human lungs

After reperfusion, the ex vivo human lungs were permitted to equilibrate to normothermic temperature. The endotracheal tube was attached to the ventilator (Servo-i, Maquet). Ventilation was initiated once lungs reached a surface temperature of 30°C and gradually increased to the following ventilatory settings: volume control mode; respiratory rate, 6 to 8 breaths min^{-1}; tidal volume, 4 to 6 ml kg^{-1}; positive end-expiratory pressure (PEEP), 5 cmH_2O; and FiO_2 21%. Atelectatic lung regions were recruited by increasing PEEP up to 10 cmH_2O and periodically performing inspiratory holds. Alveolar recruitment was performed as needed, and lungs underwent a maximum recruitment time of approximately 30 min every 4 hours, during which peak inspiratory pressures were monitored and maintained <30 cmH_2O.

Sample collection and preparation

Tissue sample collection

Before the start of each experiment, a lung map was generated assigning each lobe to an arbitrary number, as previously described (*17*). To avoid sampling bias, the location of lung wedge tissue sample collection was randomized using a random number generator (Random.org). A surgical stapler (Endo GIA Ultra, Covidien) was used to obtain lung samples at 0, 6, 12, and 18 hours of xenogeneic XC. At 24 hours of XC, wedge biopsies of all lung lobes were collected (Fig. 1C). Each wedge biopsy was sharply partitioned into specimens for histopathologic assessment and flow cytometry.

Tissue processing

Specimens were immediately fixed in 10% formalin for 24 to 72 hours, embedded in paraffin, and sectioned at a thickness of 5 μm. Sections were stained with hematoxylin and eosin, trichrome, or appropriate antibodies for immunohistochemistry and then examined under light microscopy. Additional adjacent tissue specimens were immediately placed in storage buffer (MACS Tissue Storage Solution, Miltenyi Inc.) and then digested in an enzymatic cocktail [collagenase I/dispase II (1 μg/ml) tissue or Miltenyi Multi Tissue Dissociation Kit] using a gentleMACS Octo Dissociator (Miltenyi Inc.), as previously described (*69*). For lungs 2, 3, and 4, homogenates were serially filtered through sterile gauze, 100- and 40-μm sterile filters (Thermo Fisher Scientific) to generate single-cell suspensions, which were frozen immediately in 90% fetal bovine serum/10% dimethyl sulfoxide and stored at −80°C for subsequent batched flow cytometric analysis. Lung 1 homogenates were used for protocol refinement, and insufficient cells were available for inclusion in flow cytometric analysis.

BAL fluid collection

Bronchoalveolar fluid samples were collected every 6 hours by wedging a 3.8-mm flexible video bronchoscope (aScope 3, Ambu) into a subsegmental bronchus of the left and right lower lobes of each set of lungs. Sterile normal saline (30 ml) was injected, aspirated, and collected in a sterile specimen trap (Bard). Cultures from BAL fluid samples were analyzed for bacterial and fungal growth at baseline and at the end point of XC (table S1; Antech Diagnostics). Inflammatory markers in BAL fluid were analyzed in duplicate by multiplex cytokine array (Porcine Cytokine/Chemokine 13-Plex Panel, Eve Technologies).

Immunologic analyses

Immunohistochemical staining

Human lung sections were deparaffinized and incubated in EDTA-based, pH 9 buffer (Epitope Retrieval Solution 2, BOND) for antigen retrieval for 20 min. Primary antibodies were added and incubated for 15 min to 2 hours (table S2). Secondary antibodies were diluted 1:2000 and incubated for 8 min. The BOND Polymer Refine Detection system was used for visualization. Immunostaining was performed by the Translational Pathology Research Core at Vanderbilt University Medical Center. Primary and secondary antibodies are given in table S2.

Flow cytometry

Single-cell suspensions of lung homogenate, as prepared above, were thawed and rinsed twice with phosphate-buffered saline (PBS). Up to 2 million cells per sample were incubated with a fixable live/dead marker for 30 min. Cells were rinsed twice in fluorescence-activated cell sorting (FACS) buffer (PBS + 3% fetal bovine serum) and resuspended in 100 μl of FACS buffer containing

antibodies against cell surface proteins at the listed dilutions for 30 min at 4°C (table S3). Cells were washed twice in FACS buffer and resuspended in FACS buffer containing streptavidin BUV737 for 20 min at 4°C. Cells were washed twice in FACS buffer and fixed/permeabilized for 30 min at 4°C (Tonbo Foxp3/Transcription Factor Fixation Buffer Kit, cat. no. TNB-0607-KIT). Cells were washed twice in permeabilization buffer and resuspended in 100 μl of permeabilization buffer with antibodies against intracellular proteins at the listed dilutions for 30 min at 4°C (table S3). Cells were washed twice in permeabilization buffer, resuspended in FACS buffer, and run on a flow cytometer (BD LSR II). Results were analyzed using FlowJo v10. Doublets were excluded on the basis of forward/side scatter properties, and dead cells were excluded in all analyses.

Circulating biomarkers

Blood samples were collected in blood collection tubes (BD Vacutainer) and analyzed by a diagnostic laboratory (Antech Diagnostics) for complete blood count (collected in EDTA tubes), comprehensive metabolic panel [Serum-separating tubes (SSTs)], coagulation panel, and hemolytic markers (D-dimer and fibrinogen; citrate tubes). Plasma inflammatory markers (IL-2, IL-4, IL-6, IL-8, IL-10, IL-12, IL-18, and TNF-α) were analyzed in duplicate by commercial multiplex cytokine array (Discovery Assay Pig Cytokine Array, Eve Technologies).

Complement lysis

Complement hemolytic activity was quantified using a commercial CH50 assay kit (HaemoScan) using the manufacturer's protocol. In brief, 50 μl of plasma samples were serially diluted to 4, 8, 16, 32, 64, and 128 times and incubated with 50 μl of ovine erythrocyte suspension for 30 min at 37°C. One hundred microliters of stop solution was added to all tubes, and all samples were centrifuged at 400*g* for 10 min. Supernatants (100 μl) were collected and transferred to 96-well microplates. Optical density at 415 nm was measured (Synergy HTX, BioTek). CH50 was calculated as per the manufacturer's instructions and normalized to normal human serum.

Other analyses

Functional analyses of human lungs

Blood samples were collected from the PA cannula (inflow) and PV cannula (outflow) every 6 hours with lungs ventilated at 100% FiO_2. Blood gas analysis was performed using a point-of-care analysis system (epoc, Heska). Dynamic compliance [Cdyn = TV/(PIP − PEEP)] and PaO_2/FiO_2 were calculated every 6 hours. Lung weight was obtained every 6 hours using a top-loading balance.

Transmission electron microscopy

Lung tissue samples were fixed with 2% glutaraldehyde and 2% paraformaldehyde in 0.1 M sodium cacodylate buffer (pH 7.4). Samples were then postfixed sequentially in 1% tannic acid and 1% OsO4 and enblock stained in 1% uranyl acetate. Samples were dehydrated in a grade ethanol series and embedded in EMbed 812 (Electron Microscopy Sciences). Sections with a nominal thickness of 70 nm were prepared using a Leica UC7 ultramicrotome, stained with uranyl acetate and lead citrate, and examined with a transmission electron microscope TECNAI T12 operating at 100 kV. Images were captured with an AMT NanoSprint complementary metal-oxide semiconductor camera and recorded with the AMT capture engine version 7.01.290.

Statistics and reproducibility

No data were excluded from analysis. Student's *t* tests and one-way analysis of variance (ANOVA; with Tukey's post hoc test) were performed using statistical analysis software (Prism 8.2.1, GraphPad), and $P < 0.05$ was considered statistically significant. All data are presented as means ± SD unless otherwise noted.

Supplementary Materials

This PDF file includes:

Figs. S1 to S4
Tables S1 to S3

View/request a protocol for this paper from *Bio-protocol*.

REFERENCES AND NOTES

1. S. Giwa, J. K. Lewis, L. Alvarez, R. Langer, A. E. Roth, G. M. Church, J. F. Markmann, D. H. Sachs, A. Chandraker, J. A. Wertheim, M. Rothblatt, E. S. Boyden, E. Eidbo, W. P. A. Lee, B. Pomahac, G. Brandacher, D. M. Weinstock, G. Elliott, D. Nelson, J. P. Acker, K. Uygun, B. Schmalz, B. P. Weegman, A. Tocchio, G. M. Fahy, K. B. Storey, B. Rubinsky, J. Bischof, J. A. W. Elliott, T. K. Woodruff, G. J. Morris, U. Demirci, K. G. M. Brockbank, E. J. Woods, R. N. Ben, J. G. Baust, D. Gao, B. Fuller, Y. Rabin, D. C. Kravitz, M. J. Taylor, M. Toner, The promise of organ and tissue preservation to transform medicine. *Nat. Biotechnol.* **35**, 530–542 (2017).
2. M. Valapour, C. J. Lehr, M. A. Skeans, J. M. Smith, K. Uccellini, R. Lehman, A. Robinson, A. K. Israni, J. J. Snyder, B. L. Kasiske, OPTN/SRTR 2017 annual data report: Lung. *Am. J. Transplant.* **19**, 404–484 (2019).
3. J.-Y. Chen, K. Qiao, F. Liu, B. Wu, X. Xu, G.-Q. Jiao, R.-G. Lu, H.-X. Li, J. Zhao, J. Huang, Y. Yang, X.-J. Lu, J.-S. Li, S.-Y. Jiang, D.-P. Wang, C.-X. Hu, G.-L. Wang, D.-X. Huang, G.-H. Jiao, D. Wei, S.-G. Ye, J.-A. Huang, L. Zhou, X.-Q. Zhang, J.-X. He, Lung transplantation as therapeutic option in acute respiratory distress syndrome for coronavirus disease 2019-related pulmonary fibrosis. *Chin Med J (Engl)* **133**, 1390–1396 (2020).
4. J. C. Yeung, M. Cypel, C. Chaparro, S. Keshavjee, Lung transplantation for acute COVID-19: The Toronto Lung Transplant Program experience. *CMAJ.* **193**, E1494–E1497 (2021).
5. A. Bharat, T. N. Machuca, M. Querrey, C. Kurihara, R. Garza-Castillon, S. Kim, A. Manerikar, A. Pelaez, M. Pipkin, A. Shahmohammadi, M. Rackauskas, S. R. KG, , K. R. Balakrishnan, A. Jindal, L. Schaheen, S. Hashimi, B. Buddhdev, A. Arjuna, L. Rosso, A. Palleschi, C. Lang, P. Jaksch, G. R. S. Budinger, M. Nosotti, K. Hoetzenecker, Early outcomes after lung transplantation for severe COVID-19: A series of the first consecutive cases from four countries. *Lancet Respir. Med.* **9**, 487–497 (2021).
6. J. J. Mooney, H. Hedlin, P. K. Mohabir, R. Vazquez, J. Nguyen, R. Ha, P. Chiu, K. Patel, M. R. Zamora, D. Weill, M. R. Nicolls, G. S. Dhillon, Lung quality and utilization in controlled donation after circulatory determination of death within the United States. *Am. J. Transplant.* **16**, 1207–1215 (2016).
7. E. Singh, M. Schecter, C. Towe, R. Rizwan, B. Roosevelt, J. Tweddell, M. M. Hossain, D. Morales, F. Zafar, Sequence of refusals for donor quality, organ utilization, and survival after lung transplantation. *J. Heart Lung Transplant.* **38**, 35–42 (2019).
8. A. S. Klein, E. E. Messersmith, L. E. Ratner, R. Kochik, P. K. Baliga, A. O. Ojo, Organ donation and utilization in the United States, 1999–2008. *Am. J. Transplant.* **10**, 973–986 (2010).
9. C. Divithotawela, M. Cypel, T. Martinu, L. G. Singer, M. Binnie, C.-W. Chow, C. Chaparro, T. K. Waddell, M. de Perrot, A. Pierre, K. Yasufuku, J. C. Yeung, L. Donahoe, S. Keshavjee, J. M. Tikkanen, Long-term outcomes of lung transplant with ex vivo lung perfusion. *JAMA Surg.* **154**, 1143–1150 (2019).
10. T. N. Machuca, M. Cypel, Ex vivo lung perfusion. *J. Thorac. Dis.* **6**, 1054 (2014).
11. XVIVO Perfusion, Novel Lung Trial: Normothermic Ex Vivo Lung Perfusion (Evlp) As An Assessment Of Extended/Marginal Donor Lungs, *ClinicalTrials.gov*(2020); www.clinicaltrials.gov/ct2/show/NCT01365429.
12. G. Loor, B. T. Howard, J. R. Spratt, L. M. Mattison, A. Panoskaltsis-Mortari, R. Z. Brown, T. L. Iles, C. M. Meyer, H. Helms, A. Price, P. A. Iaizzo, Prolonged EVLP using OCS lung: Cellular and acellular perfusates. *Transplantation* **101**, 2303–2311 (2017).
13. J. R. Spratt, L. M. Mattison, P. A. Iaizzo, R. Z. Brown, H. Helms, T. L. Iles, B. Howard, A. Panoskaltsis-Mortari, G. Loor, An experimental study of the recovery of injured porcine lungs with prolonged normothermic cellular ex vivo lung perfusion following donation after circulatory death. *Transpl. Int.* **30**, 932–944 (2017).
14. J. D. O'Neill, B. A. Guenthart, J. Kim, S. Chicotka, D. Queen, K. Fung, C. Marboe, A. Romanov, S. X. L. Huang, Y. W. Chen, H. W. Snoeck, M. Bacchetta, G. Vunjak-Novakovic, Cross-

circulation for extracorporeal support and recovery of the lung. *Nat. Biomed. Eng.* **1**, 0037 (2017).
15. B. A. Guenthart, J. D. O'Neill, J. Kim, D. Queen, S. Chicotka, K. Fung, M. Simpson, R. Donocoff, M. Salna, C. C. Marboe, K. Cunningham, S. P. Halligan, H. M. Wobma, A. E. Hozain, A. Romanov, G. Vunjak-Novakovic, M. Bacchetta, Regeneration of severely damaged lungs using an interventional cross-circulation platform. *Nat. Commun.* **10**, 1985 (2019).
16. A. E. Hozain, Y. Tipograf, M. R. Pinezich, K. M. Cunningham, R. Donocoff, D. Queen, K. Fung, C. C. Marboe, B. A. Guenthart, J. D. O'Neill, G. Vunjak-Novakovic, M. Bacchetta, Multiday maintenance of extracorporeal lungs using cross-circulation with conscious swine. *J. Thorac. Cardiovasc. Surg.* **159**, 1640–1653.e18 (2020).
17. A. E. Hozain, J. D. O'Neill, M. R. Pinezich, Y. Tipograf, R. Donocoff, K. M. Cunningham, A. Tumen, K. Fung, R. Ukita, M. T. Simpson, J. A. Reimer, E. C. Ruiz, D. Queen, J. W. Stokes, N. L. Cardwell, J. Talackine, J. Kim, H. W. Snoeck, Y. W. Chen, A. Romanov, C. C. Marboe, A. D. Griesemer, B. A. Guenthart, M. Bacchetta, G. Vunjak-Novakovic, Xenogeneic cross-circulation for extracorporeal recovery of injured human lungs. *Nat. Med.* **26**, 1102–1113 (2020).
18. W. K. Wu, A. Tumen, J. W. Stokes, R. Ukita, A. Hozain, M. Pinezich, J. D. O'Neill, M. J. Lee, J. A. Reimer, C. R. Flynn, J. R. Talackine, N. L. Cardwell, C. Benson, G. Vunjak-Novakovic, S. P. Alexopoulos, M. Bacchetta, Cross-circulation for extracorporeal liver support in a swine model. *ASAIO J.* **68**, 561–570 (2021).
19. R. N. Pierson, A. Dorling, D. Ayares, M. A. Rees, J. D. Seebach, J. A. Fishman, B. J. Hering, D. K. C. Cooper, Current status of xenotransplantation and prospects for clinical application. *Xenotransplantation* **16**, 263–280 (2009).
20. D. K. C. Cooper, V. Satyananda, B. Ekser, D. J. Van Der Windt, H. Hara, M. B. Ezzelarab, H. J. Schuurman, Progress in pig-to-non-human primate transplantation models (1998–2013): A comprehensive review of the literature. *Xenotransplantation* **21**, 397–419 (2014).
21. M. Längin, T. Mayr, B. Reichart, S. Michel, S. Buchholz, S. Guethoff, A. Dashkevich, A. Baehr, S. Egerer, A. Bauer, M. Mihalj, A. Panelli, L. Issl, J. Ying, A. K. Fresch, I. Buttgereit, M. Mokelke, J. Radan, F. Werner, I. Lutzmann, S. Steen, T. Sjöberg, A. Paskevicius, L. Qiuming, R. Sfriso, R. Rieben, M. Dahlhoff, B. Kessler, E. Kemter, K. Klett, R. Hinkel, C. Kupatt, A. Falkenau, S. Reu, R. Ellgass, R. Herzog, U. Binder, G. Wich, A. Skerra, D. Ayares, A. Kind, U. Schönmann, F. J. Kaup, C. Hagl, E. Wolf, N. Klymiuk, P. Brenner, J. M. Abicht, Consistent success in life-supporting porcine cardiac xenotransplantation. *Nature* **564**, 430–433 (2018).
22. R. A. Montgomery, S. A. Mehta, B. Parent, A. Griesemer, Next steps for the xenotransplantation of pig organs into humans. *Nat. Med.* **28**, 1533–1536 (2022).
23. B. A. Macher, U. Galili, The Galα1,3Galβ1,4GlcNAc-R (α-Gal) epitope: A carbohydrate of unique evolution and clinical relevance. *Biochim. Biophys. Acta* **1780**, 75–88 (2008).
24. U. Galili, F. Anaraki, A. Thall, C. Hill-Black, M. Radic, One percent of human circulating B lymphocytes are capable of producing the natural anti-gal antibody. *Blood* **82**, 2485–2493 (1993).
25. D. K. C. Cooper, A. H. Good, E. Koren, R. Oriol, A. J. Malcolm, R. M. Ippolito, F. A. Neethling, Y. Ye, E. Romano, N. Zuhdi, Identification of α-galactosyl and other carbohydrate epitopes that are bound by human anti-pig antibodies: Relevance to discordant xenografting in man. *Transpl. Immunol.* **1**, 198–205 (1993).
26. A. G. Rose, D. K. C. Cooper, Venular thrombosis is the key event in the pathogenesis of antibody-mediated cardiac rejection. *Xenotransplantation* **7**, 31–41 (2000).
27. G. M. Hansch, C. H. Hammer, P. Vanguri, M. L. Shin, Homologous species restriction in lysis of erythrocytes by terminal complement proteins. *Proc. Natl. Acad. Sci. U.S.A.* **78**, 5118–5121 (1981).
28. A. Griesemer, K. Yamada, M. Sykes, Xenotransplantation: Immunological hurdles and progress toward tolerance. *Immunol. Rev.* **258**, 241–258 (2014).
29. B. P. Morgan, C. W. Van Den Berg, C. L. Harris, '"Homologous restriction"' in complement lysis: Roles of membrane complement regulators. *Xenotransplantation* **12**, 258–265 (2005).
30. H. C. Tai, X. Zhu, H. Hara, Y. J. Lin, M. Ezzelarab, C. Long, S. Ball, D. Ayares, D. K. C. Cooper, The pig-to-primate immune response: Relevance for xenotransplantation. *Xenotransplantation* **14**, 227–235 (2007).
31. J. Smart, B. Casale, TNF-alpha-induced transendothelial neutrophil migration is IL-8 dependent. *Am. J. Physiol.* **266**, L238–L245 (1994).
32. S. J. Smart, T. B. Casale, Pulmonary epithelial cells facilitate TNF-α-induced neutrophil chemotaxis. A role for cytokine networking. *J. Immunol.* **152**, 4087–4094 (1994).
33. E. Gianchecchi, D. V. Delfino, A. Fierabracci, Natural killer cells: Potential biomarkers and therapeutic target in autoimmune diseases? *Front. Immunol.* **12**, 616853 (2021).
34. A. M. Abel, C. Yang, M. S. Thakar, S. Malarkannan, Natural killer cells: Development, maturation, and clinical utilization. *Front. Immunol.* **9**, 1869 (2018).
35. C. Summers, S. M. Rankin, A. M. Condliffe, N. Singh, A. M. Peters, E. R. Chilvers, Neutrophil kinetics in health and disease. *Trends Immunol.* **31**, 318–324 (2010).
36. R. Fischel, A. Matas, J. Platt, E. Perry, H. Noreen, S. Shumway, R. Bolman, Cardiac xenografting in the pig-to-rhesus monkey model: Manipulation of antiendothelial antibody prolongs survival. *J. Heart Lung Transplant.* **11**, 965–973 (1992).
37. S. S. Lin, M. J. Hanaway, G. V. Gonzalez-Stawinski, C. L. Lau, W. Parker, R. D. Davis, G. W. Byrne, L. E. Diamond, J. S. Logan, J. L. Platt, The role of anti-Galα1-3gal antibodies in acute vascular rejection and accommodation of xenografts. *Transplantation* **70**, 1667–1674 (2000).
38. R. J. Lynch, J. L. Platt, Accommodation in renal transplantation: Unanswered questions. *Curr. Opin. Organ Transplant.* **15**, 481–485 (2010).
39. D. Kervella, S. le Bas-Bernardet, S. Bruneau, G. Blancho, Protection of transplants against antibody-mediated injuries: from xenotransplantation to allogeneic transplantation, mechanisms and therapeutic insights. *Front. Immunol.* **13**, 932242 (2022).
40. J. L. Platt, M. Cascalho, Accommodation in allogeneic and xenogeneic organ transplantation: Prevalence, impact, and implications for monitoring and for therapeutics. *Hum. Immunol.* **84**, 5–17 (2023).
41. A. Dorling, Are anti-endothelial cell antibodies a pre-requisite for the acute vascular rejection of xenografts? *Xenotransplantation* **10**, 16–23 (2003).
42. S. M. Black, B. A. Benson, D. Idossa, G. M. Vercellotti, A. P. Dalmasso, Protection of porcine endothelial cells against apoptosis with interleukin-4. *Xenotransplantation* **18**, 343–354 (2011).
43. Q. Li, H. Hara, Z. Zhang, M. E. Breimer, Y. Wang, D. K. C. Cooper, Is sensitization to pig antigens detrimental to subsequent allotransplantation? *Xenotransplantation* **25**, e12393 (2018).
44. M. Hryhorowicz, J. Zeyland, R. Słomski, D. Lipiński, Genetically modified pigs as organ donors for xenotransplantation. *Mol. Biotechnol.* **59**, 435–444 (2017).
45. S. Le Bas-Bernardet, I. Anegon, G. Blancho, Progress and prospects: Genetic engineering in xenotransplantation. *Gene Therapy* **15**, 1247–1256 (2008).
46. P. M. Porrett, B. J. Orandi, V. Kumar, J. Houp, D. Anderson, A. Cozette Killian, V. Hauptfeld-Dolejsek, D. E. Martin, S. Macedon, N. Budd, K. L. Stegner, A. Dandro, M. Kokkinaki, K. V. Kuravi, R. D. Reed, H. Fatima, J. T. Killian, G. Baker, J. Perry, E. D. Wright, M. D. Cheung, E. N. Erman, K. Kraebber, T. Gamblin, L. Guy, J. F. George, D. Ayares, J. E. Locke, First clinical-grade porcine kidney xenotransplant using a human decedent model. *Am. J. Transplant.* **22**, 1037–1053 (2022).
47. K. Kuwaki, Y.-L. Tseng, F. J. M. F. Dor, A. Shimizu, S. L. Houser, T. M. Sanderson, C. J. Lancos, D. D. Prabharasuth, J. Cheng, K. Moran, Y. Hisashi, N. Mueller, K. Yamada, J. L. Greenstein, R. J. Hawley, C. Patience, M. Awwad, J. A. Fishman, S. C. Robson, H.-J. Schuurman, D. H. Sachs, D. K. C. Cooper, Heart transplantation in baboons using α1,3-galactosyltransferase gene-knockout pigs as donors: Initial experience. *Nat Med.* **11**, 29–31 (2005).
48. R. A. Montgomery, J. M. Stern, B. E. Lonze, V. S. Tatapudi, M. Mangiola, M. Wu, E. Weldon, N. Lawson, C. Deterville, R. A. Dieter, B. Sullivan, G. Boulton, B. Parent, G. Piper, P. Sommer, S. Cawthon, E. Duggan, D. Ayares, A. Dandro, A. Fazio-Kroll, M. Kokkinaki, L. Burdorf, M. Lorber, J. D. Boeke, H. Pass, B. Keating, A. Griesemer, N. M. Ali, S. A. Mehta, Z. A. Stewart, Results of two cases of pig-to-human kidney xenotransplantation. 386, 1889–1898 (2022).
49. M. Rothblatt, Commentary on achievement of first life-saving xenoheart transplant. *Xenotransplantation* **29**, e12746 (2022).
50. B. P. Griffith, C. E. Goerlich, A. K. Singh, M. Rothblatt, C. L. Lau, A. Shah, M. Lorber, A. Grazioli, K. K. Saharia, S. N. Hong, S. M. Joseph, D. Ayares, M. M. Mohiuddin, Genetically modified porcine-to-human cardiac xenotransplantation. *N. Engl. J. Med.* **387**, 35–44 (2022).
51. F. H. Bach, H. Winkler, C. Ferran, W. W. Hancock, S. C. Robson, Delayed xenograft rejection. *Immunol. Today* **17**, 379–384 (1996).
52. K. Kiernan, I. Harnden, M. Gunthart, C. Gregory, J. Meisner, M. Kearns-Jonker, The anti-non-gal xenoantibody response to xenoantigens on gal knockout pig cells is encoded by a restricted number of germline progenitors. *Am. J. Transplant.* **8**, 1829–1839 (2008).
53. B. C. Baumann, G. Stussi, K. Huggel, R. Rieben, J. D. Seebach, Reactivity of human natural antibodies to endothelial cells from Galα(1,3)Gal-deficient pigs. *Transplantation* **83**, 193–201 (2007).
54. M. Ezzelarab, H. Hara, J. Busch, P. P. M. Rood, X. Zhu, Z. Ibrahim, S. Ball, D. Ayares, M. Awwad, D. K. C. Cooper, Antibodies directed to pig non-Gal antigens in naïve and sensitized baboons. *Xenotransplantation* **13**, 400–407 (2006).
55. K. Morozumi, T. Kobayashi, T. Usami, T. Oikawa, Y. Ohtsuka, M. Kato, O. Takeuchi, K. Koyama, H. Matsuda, I. Yokoyama, H. Takagi, Significance of histochemical expression of Hanganutziu-Deicher antigens in pig, baboon and human tissues. *Transplant. Proc.* **31**, 942–944 (1999).
56. H. Pan, A. Gazarian, I. Mollet, V. Mathias, V. Dubois, M. Sobh, S. Buff, J. M. Dubernard, M. Michallet, M. C. Michallet, Lymphodepletive effects of rabbit anti-pig thymocyte globulin in neonatal swines. *Transpl. Immunol.* **39**, 74–83 (2016).
57. J. A. Emamaullee, S. Merani, C. P. Larsen, A. M. J. Shapiro, Belatacept and basiliximab diminish human antiporcine xenoreactivity and synergize to inhibit alloimmunity. *Transplantation* **85**, 118–124 (2008).

58. V. Fahradyan, M. J. Annunziata, S. Said, M. Rao, H. Shah, C. Ordenana, F. A. Papay, A. Rampazzo, B. B. Gharb, Leukoreduction in ex vivo perfusion circuits: comparison of leukocyte depletion efficiency with leukocyte filters. *Perfusion* **35**, 853–860 (2020).
59. M. Mendicino, J. Ramsoondar, C. Phelps, T. Vaught, S. Ball, T. Leroith, J. Monahan, S. Chen, A. Dandro, J. Boone, P. Jobst, A. Vance, N. Wertz, Z. Bergman, X.-Z. Sun, I. Polejaeva, J. Butler, Y. Dai, D. Ayares, K. Wells, Á. J. Ramsoondar, Á. C. Phelps, Á. T. Vaught, Á. S. Ball, Á. J. Monahan, Á. S. Chen, Á. A. Dandro, Á. J. Boone, Á. P. Jobst, Á. A. Vance, Á. I. Polejaeva, Y. Dai, Á. D. Ayares, Á. K. Wells, T. Leroith, N. Wertz, Á. Z. Bergman, Á. X.-Z. Sun, Á. J. Butler, K. Wells, Generation of antibody- and B cell-deficient pigs by targeted disruption of the J-region gene segment of the heavy chain locus. *Transgenic Res.* **20**, 625–641 (2011).
60. A. N. Boettcher, C. L. Loving, J. E. Cunnick, C. K. Tuggle, Development of severe combined immunodeficient (SCID) pig models for translational cancer modeling: Future insights on how humanized SCID pigs can improve preclinical cancer research. *Front. Oncol.* **8**, 559 (2018).
61. C. Haihua, W. Wei, H. Kun, L. Yuanli, L. Fei, Cobra venom factor-induced complement depletion protects against lung ischemia reperfusion injury through alleviating blood-air barrier damage. *Sci. Rep.* **8**, 10346 (2018).
62. C. G. Cochrane, J. Hans, B. S. Aikin, Depletion of plasma complement in vivo by a protein of cobra venom: Its effect on various immunologic reactions. *J. Immunol.* **105**, 55–69 (1970).
63. L. Munshi, S. Keshavjee, M. Cypel, Donor management and lung preservation for lung transplantation. *Lancet Respir. Med.* **1**, 318–328 (2013).
64. M. Cypel, J. C. Yeung, M. Liu, M. Anraku, F. Chen, W. Karolak, M. Sato, J. Laratta, S. Azad, M. Madonik, C.-W. Chow, C. Chaparro, M. Hutcheon, L. G. Singer, A. S. Slutsky, K. Yasufuku, M. de Perrot, A. F. Pierre, T. K. Waddell, S. Keshavjee, Normothermic ex vivo lung perfusion in clinical lung transplantation. *N. Engl. J. Med.*. **364**, 1431–1440 (2011).
65. M. Cypel, J. C. Yeung, S. Keshavjee, Introducing the concept of semielective lung transplantation through the use of ex vivo lung perfusion. *J. Thorac. Cardiovasc. Surg.* **156**, 2350–2352 (2018).
66. B. A. Guenthart, J. D. O'Neill, M. Bacchetta, Cannulation strategies in ex vivo lung perfusion. *ASAIO J.* **68**, e222 (2022).
67. M. Cypel, J. C. Yeung, S. Hirayama, M. Rubacha, S. Fischer, M. Anraku, M. Sato, S. Harwood, A. Pierre, T. K. Waddell, M. de Perrot, M. Liu, S. Keshavjee, Technique for prolonged normothermic ex vivo lung perfusion. *J. Heart Lung Transplant.* **27**, 1319–1325 (2008).
68. W. K. Wu, B. A. Guenthart, J. D. O'Neill, A. E. Hozain, Y. Tipograf, R. Ukita, J. W. Stokes, Y. J. Patel, M. Pinezich, J. R. Talackine, N. L. Cardwell, K. Fung, G. Vunjak-Novakovic, M. Bacchetta, Technique for xenogeneic cross-circulation to support human donor lungs ex vivo. *J. Heart Lung Transplant.* **42**, 335–344 (2022).
69. A. C. Habermann, A. J. Gutierrez, L. T. Bui, S. L. Yahn, N. I. Winters, C. L. Calvi, L. Peter, M. I. Chung, C. J. Taylor, C. Jetter, L. Raju, J. Roberson, G. Ding, L. Wood, J. M. S. Sucre, B. W. Richmond, A. P. Serezani, W. J. McDonnell, S. B. Mallal, M. J. Bacchetta, J. E. Loyd, C. M. Shaver, L. B. Ware, R. Bremner, R. Walia, T. S. Blackwell, N. E. Banovich, J. A. Kropski, Single-cell RNA sequencing reveals profibrotic roles of distinct epithelial and mesenchymal lineages in pulmonary fibrosis. *Sci. Adv.* **6**, eaba1972 (2020).

Acknowledgments: We thank the following collaborators and supporters: Vanderbilt Light Surgical Research Laboratory staff J. Diaz, J. Adcock, M. S. Fultz, and M. C. VanRooyen for technical support and research infrastructure; Vanderbilt Translational Pathology Shared Resource (TPSR) staff, including A. Joritz and M. Wilkes for laboratory pathology support (supported by the NCI/NIH Cancer Center Support Grant 5P30 CA68485-19); TPSR Research Histology for immunohistochemistry services and use of the Leica Bond RX (supported by the Shared Instrumentation Grant S10 OD023475-01A1); Vanderbilt Cell Imaging Shared Resource for transmission electron microscopy processing and imaging services (supported by NIH grants CA68485, DK20593, DK58404, DK59637, and EY08126); Tennessee Donor Services, DCI Inc., and Lung Bioengineering for organ research infrastructure; S. Scholl and A. Dutton for administrative support; and W. W. Wade for tissue and sample transport assistance. **Funding:** W.K.W. is supported by the Burroughs Wellcome Fund Physician-Scientist Institutional Award to Vanderbilt University (ID: 1018894). C.M.S. is supported by NIH HL136888. M.B. is supported through NIH HL140231, CDMRP PR212237, and the H. William Scott, Jr. Chair in Surgery Foundation. **Author contributions:** W.K.W., M.T.S., J.W.S., C.M.S., and M.B. conceived the study. W.K.W., M.T.S., J.W.S., R.U., Y.J.P., S.P.A., C.M.S., and M.B. planned the experiments. W.K.W., J.W.S., R.U., Y.J.P., M.C., S.R.L., J.R.T., N.L.C., E.M.S., M.M., C.B., and C.T.D. implemented the experiments and collected data. W.K.W., M.T.S., C.M.S., and M.B. coordinated the data analysis efforts. W.K.W., M.T.S., N.L.C., C.L., C.M.S., and M.B. analyzed the data. W.K.W. primarily drafted the manuscript with input from all authors. W.K.W., M.T.S., J.W.S., R.U., S.P.A., C.M.S., and M.B. provided critical feedback and helped shape the research, analysis, and manuscript. **Competing interests:** M.B. is an inventor on a patent related to this work filed by Columbia University (no. WO2018013849A1, filed 13 July 2017, published 18 January 2018). W.K.W., J.W.S., R.U., S.P.A., and M.B. are inventors on a patent application related to this work filed by Vanderbilt University (no. 63/165,773, filed 25 March 2021). The authors declare that they have no other competing interests. **Data and materials availability:** All data needed to evaluate the conclusions in the paper are present in the paper and/or the Supplementary Materials. Preliminary results included here were presented at the 42nd Annual Meeting and Scientific Sessions of the International Society for Heart and Lung Transplantation (27 to 30 April 2022).

Submitted 6 September 2022
Accepted 27 February 2023
Published 31 March 2023
10.1126/sciadv.ade7647